Available online at www.sciencedirect.com
ScienceDirect
Journal of Organometallic Chemistry 693 (2008) 1081–1095
Journal of Organometallic Chemistry
www.elsevier.com/locate/jorganchem

Heterocarbenoids of germanium and tin and their polyhedral oxidation products: The case for thermodynamic product control in Group 14 chalcogenides

Ingo Schranz [a], Luke Grocholl [a], Christopher J. Carrow [a], Lothar Stahl [a,*], Richard J. Staples [b]

[a] Department of Chemistry, University of North Dakota, Grand Forks, ND 58202-9024, United States
[b] Department of Chemistry and Chemical Biology, Harvard University, Cambridge, MA 02138, United States

Received 18 September 2007; received in revised form 28 December 2007; accepted 28 December 2007
Available online 8 January 2008

Abstract

The polycyclic Group 14 amides $[P(\mu\text{-}N^tBu)_2P(^tBuN)_2]M$, M = Ge (**4**), Sn (**5**) were synthesized from *cis*-$[P(\mu\text{-}N^tBu)_2P(^tBuN\text{-}Li\cdot THF)_2]$ and $GeCl_2\cdot$dioxane or $SnCl_2$, respectively. Oxidation of these heterocarbenoids or of the analogous diazastannylene $[MeSi(\mu\text{-}^tBuN)_2SiMe(^tBuN)_2]Sn$ with O_2, S_8 and Se_n furnished the chalcogenides $\{[P(\mu\text{-}N^tBu)_2P(^tBuN)_2]GeO\}_2$ (**6**), $\{[P(\mu\text{-}N^tBu)_2\text{-}P(^tBuN)_2]SnE\}_2$, E = O (**7**), S (**8**), Se (**9**), $\{[SP(\mu\text{-}N^tBu)_2P(^tBuN)_2]SnS\}_2$ (**10**), and $\{[MeSi(\mu\text{-}^tBuN)_2SiMe(^tBuN)_2]SnE\}_2$, E = S (**11**), Se (**12**), respectively. All products (**6–12**) were shown by single-crystal X-ray methods to consist of dimeric molecules with central $(M\text{–}E)_2$ rings, M = Group 14 element, E = chalcogen. The exclusive formation of dimeric compounds with bridging M–E–M bonds, vs. alternative monomeric structures with terminal M=E bonds, is rationalized in terms of the thermodynamic favorability of the dimers. The case is made that most, if not all, currently known Group 14 chalcogenides, even those labeled "kinetically stabilized", are really thermodynamic products.

Keywords: Heterocarbenoids; Germylene; Stannylene; Group 14 chalcogenides; Base-stabilized double bonds; Kinetically-stabilized double bonds

1. Introduction

N-Heterocyclic carbenes (NHCs), such as the imidazol-2-ylidenes **A** in Chart 1, are remarkably stable, divalent, two-coordinate carbon compounds [1–4]. Although these molecules were first reported in the 1960s [5–7], they have only recently become the focus of intense research interests because of their outstanding ligand properties [8–11]. Thus, heterocarbenes are successful ligands in a wide range of catalytic reactions, such as Heck and Suzuki couplings [12–14], olefin metathesis [15–18], and C–H bond activation [19], to name a few.

While less well known than heterocarbenes, the heterocarbene analogues of the heavier Group 14 elements (E = Ge, Sn, Pb, **B**) are also a mature research area, dating back to the pioneering work of Lappert and coworkers in the early 1970s [20,21]. Related N-heterocyclic Group 14 carbenoids, like **C** [22] and **D** [23], were reported slightly later by Veith et al. and those of structure type **E** somewhat later still by Herrmann, Denk, and West [24]. All of these compounds are readily synthesized from the Group 14 halides and the appropriate lithium amides or -diamides, and like NHCs, these carbenoids have a well-developed coordination chemistry with transition metals [25–29].

One of the most obvious transformations of the heterocarbene analogues **B–E**, namely their oxidation with chalcogens, was not investigated until Veith et al. reported the reactions of the germanium(II) bis(*tert*-butylamido)cyclodisilazane **1** (Scheme 1) with oxygen and sulfur [30,31]. In

* Corresponding author. Fax: +1 701 777 2331.
E-mail address: lstahl@chem.und.edu (L. Stahl).

0022-328X/$ - see front matter © 2008 Elsevier B.V. All rights reserved.
doi:10.1016/j.jorganchem.2007.12.031

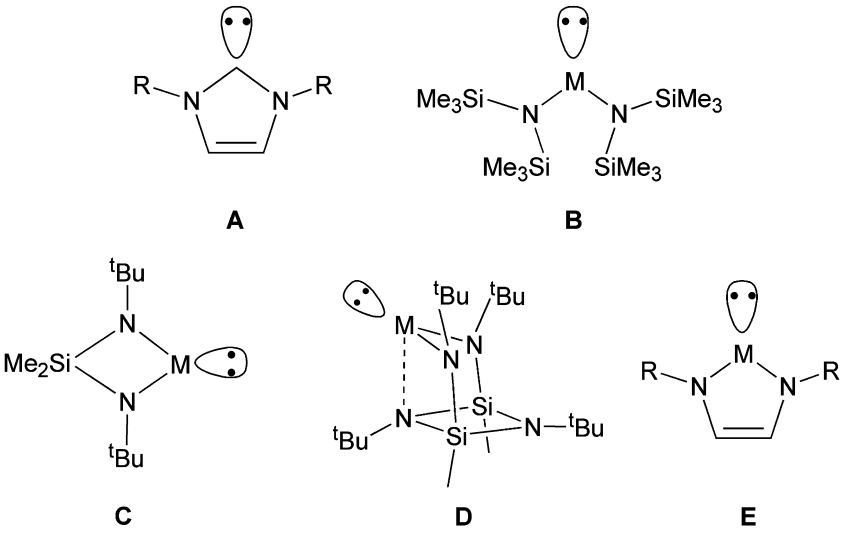

Chart 1.

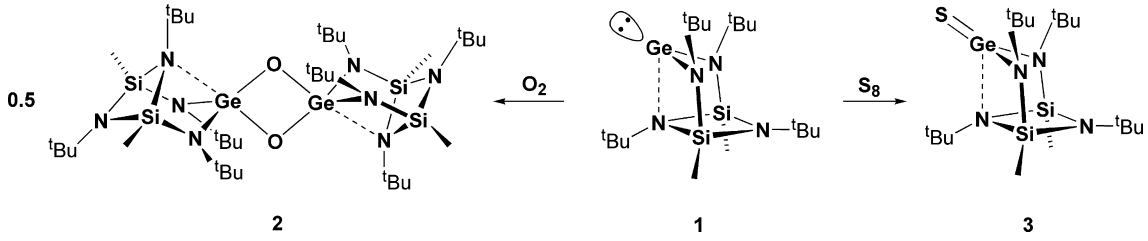

Scheme 1.

both reactions, the germylene was transformed cleanly to the corresponding germanium(IV) chalcogenide. However, while the oxide crystallized dimeric with a bridging (Ge–O)$_2$ rhombus (**2**), the sulfide was monomeric (**3**), featuring the shortest terminal Ge=S bond (2.062(3) Å) reported to that date. The unusual stability of the terminal Ge=S bond was attributed to the intramolecular Lewis base-stabilization originating from one of the MeSi(μ-^{t}BuN)$_2$SiMe heterocycle's nitrogen atoms. Since this donor interaction is present in both, monomer **3** and dimer **2**, the authors were presumably implying that the substantially shorter donor bond in **3** (2.050(5) Å) vs. that in **2** (2.396(6) Å) is suggestive of a stronger interaction in the germanium sulfide, which therefore remained monomeric.

The discovery of this first terminal Group 14 chalcogenide bond in a molecular compound spawned research on related Group 14 chalcogenides – Chart 2 displays some of these – which showed that such double bonds between Group 14 metal(loids) and chalcogens are less difficult to stabilize than had been imagined [32–56].

Compounds **2** and **3** constitute the two limiting structures of Group 14 chalcogenides, namely dimers (or oligomers) with bridging chalcogen atoms (**2**) and monomers with a doubly-bonded, terminal chalcogen atom (**3**). While compounds of both structural types are potentially useful as precursors for Group 14/16 materials, terminal metal-chalcogenides of the heavier Group 14 elements have also elicited interest from chemists for their unusual structure and bonding. Such compounds violate the "double bond rule", namely, that elements past the 2nd period of the periodic table are not involved in double-bond formation [57].

We have been investigating the main-group and transition-metal chemistry of the bis(amino)cyclodiphosphazane **L**, which is isoelectronic with the bis(*tert*-butylamido)cyclodisilazane ligand **M** of **1**–**3**. The lone difference between these two heterocyclic ligands is the substitution of both MeSi groups with trivalent phosphorus atoms. Phosphorus is slightly smaller (1.06 Å) than silicon (1.11 Å) and also somewhat more electronegative than the metalloid, namely 2.19 vs. 1.90 on the Pauling scale [58]. The structures adopted by the germanium chalcogenides **2** and **3** are obviously influenced by minor steric and electronic factors. We therefore wondered if even the small ligand modifications on going from **M** to **L** would be sufficient to favor Group 14 chalcogenides with terminal M=E bonds (see Chart 3).

Below we report on the syntheses and structures of germanium and tin heterocarbenoids and their oxidations by elemental chalcogens, with a particular emphasis on the structures of the ensuing chalcogenides. In our discussion of these compounds we will attempt to show that the structures adopted by Group 14 chalcogenides presented herein, and those of Group 14 chalcogenides in general, are the result of thermodynamic, rather than kinetic, factors. The

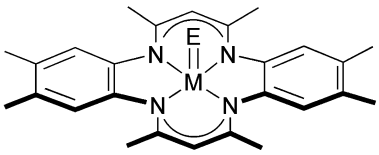

M = Ge; E = S, Se, Te
M = Sn; E = S, Se

F

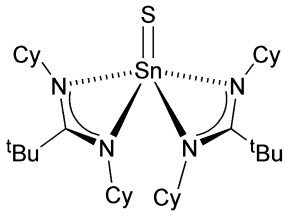

G

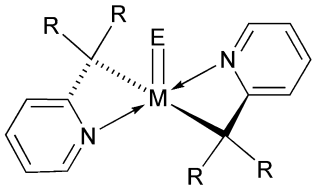

M = Ge, Sn; E = S, Se, Te

H

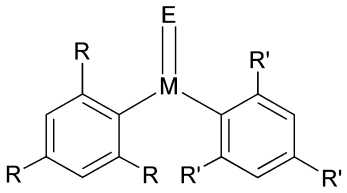

M = Si, Ge, Sn; E = S, Se, Te

I

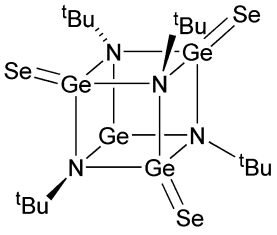

J

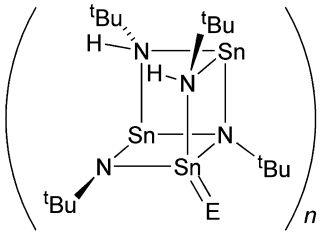

E = S(n = 2), Se(n =1, 2), Te(n = 1)

K

Chart 2.

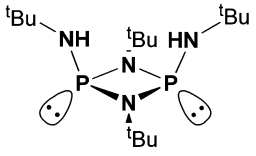

L

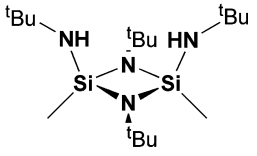

M

Chart 3.

commonly used terms "kinetically-stabilized" and "base-stabilized" double bonds to differentiate seemingly different types of terminal Group 14 chalcogenides are therefore, in our opinion, not useful and potentially misleading.

2. Results

2.1. Syntheses

Germanium(II) chloride mono-dioxane and tin(II) chloride reacted with *cis*-[P(μ-N^{t}Bu)$_2$P(^{t}BuNLi · THF)$_2$] [59], Scheme 2, to afford, respectively, the germylene *cis*-[P(μ-N^{t}Bu)$_2$P(^{t}BuN)$_2$]Ge (**4**) and the stannylene *cis*-[P(μ-N^{t}Bu)$_2$-P(^{t}BuN)$_2$]Sn (**5**) as analytically-pure, light-yellow solids. Efforts to isolate these compounds in single crystal form suitable for X-ray diffraction studies failed, just as they had for the cyclodisilazane analogues.

While the multinuclear (^{1}H, ^{13}C, ^{31}P) NMR studies of both **4** and **5** do not provide definitive answers regarding the solution structures of these heterocarbenoids, they strongly suggest that these compounds are analogues of **1**. Thus, the ^{1}H NMR spectra showed only two sharp singlets; for the tertiary butyl substituents of the amido and imino nitrogen atoms, respectively. These spectra do not change significantly, even at −80 °C, but we believe them to be due to fluxional solution structures rather than symmetrical ground-state structures. Asymmetric ground state structures in which the Group 14 element is slightly displaced from the molecular center, as shown in Scheme 2, have been observed for all X-ray structurally-characterized derivatives of **L**. Based on the variable-temperature NMR

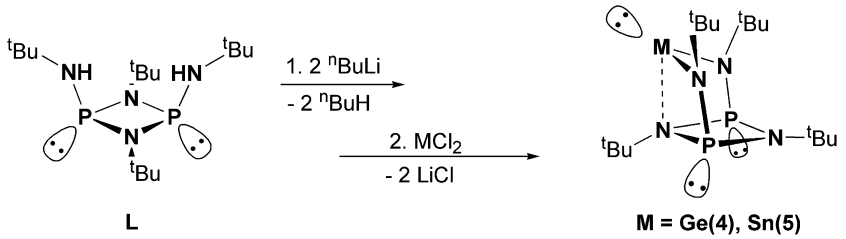

Scheme 2.

data we estimate an upper limit for the activation energies of the equilibrating motion of ca. 6 kcal mol^{-1}.

Despite their electron-deficiency both **4** and **5** are rapidly oxidized by elemental chalcogens (Scheme 3), the reaction of the germanium compound being significantly faster than that of the tin analogue. Thus, when a stream of dioxygen was bubbled through a solution of **4**, an insoluble, white solid (**6**) formed almost instantly.

The analogous O_2 oxidation of $[P(\mu\text{-}N^tBu)_2P(^tBuN)_2]Sn$, **5**, proceeded expectedly slower than that of the diazagermylene, but was still comparatively fast, while the oxidations of the diazastannylene with sulfur and grey selenium required prolonged heating. In all three oxidations rather insoluble, crystalline solids were recovered in high yields, suggestive of dimeric, rather than monomeric, structures. The dimeric nature of these compounds was confirmed by mass spectral data, which showed molecular ion peaks for the dimers. Prolonged interaction of the stannylene **5** with excess sulfur at elevated temperatures caused one of the phosphorus atoms of the ligand to become oxidized also, (Scheme 4) furnishing the isomeric cyclodiphosph(III/V)azane derivatives **10a** and **10b**.

The mass spectral and microanalytical data of **10** demonstrated that only two of the four phosphorus atoms had been oxidized. Based on the multitude of NMR signals we suspected that both the *trans*-(**10a**) and the *cis*-isomer (**10b**) were present, and this assumption was corroborated by the X-ray crystallographic data.

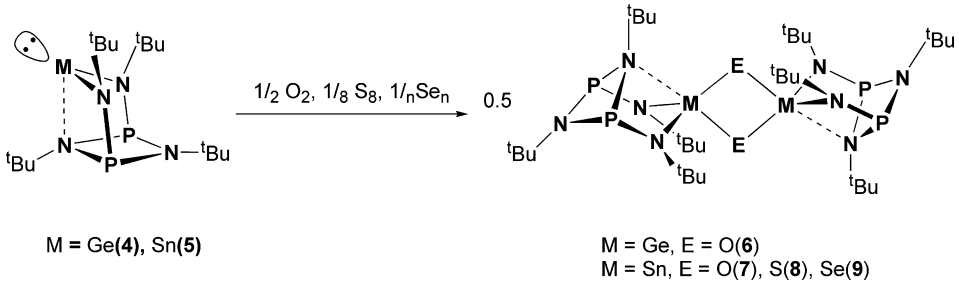

Scheme 3.

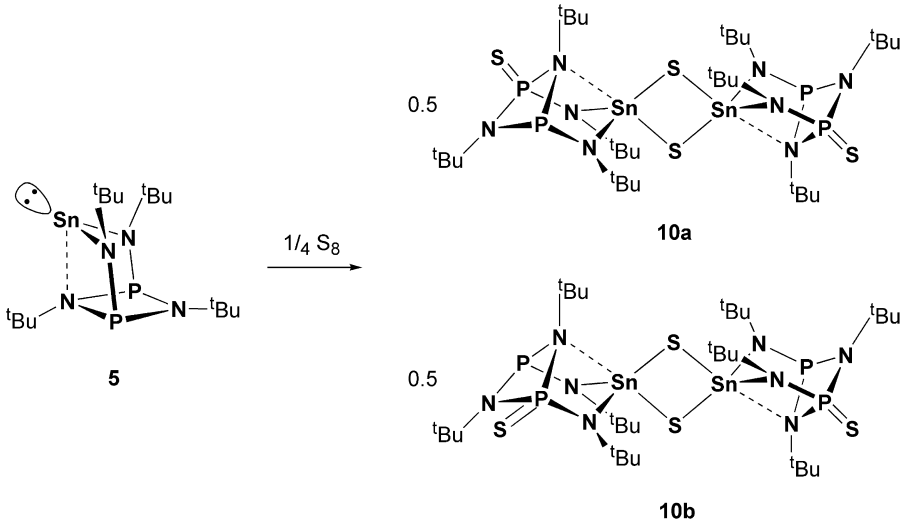

Scheme 4.

Although the stannylene analogue of **1**, namely [MeSi(μ-N^{t}Bu)$_2$SiMe(^{t}BuN)$_2$]Sn, had been reported previously [23], its sulfide and selenide derivatives were unknown. To have these compounds available for structural comparisons, we synthesized them as shown in Scheme 5, and obtained the sulfide (**11**) and the selenide (**12**) derivatives as relatively soluble, light-yellow and colorless crystalline solids, respectively.

2.2. Solid-state structures

With the exception of **4** and **5** and the cyclodisilazane-based **11** and **12**, all of the title compounds have very low solubilities in conventional solvents. Their structural characterizations thus rest mainly on X-ray diffraction studies. A single-crystal study of **6** showed that, like the cyclodisilazane analogue, this germanium oxide is dimeric, but unlike **2** it crystallizes in the cubic crystal system, space group *Pa*−3, with the four dimeric molecules of the unit cell located on threefold rotoinversion (−3) axes [60]. The molecular symmetry is not commensurate with such a high site-symmetry, however, indicating a disordered solid-state structure. This disorder naturally limits the precision of the bond parameters derived from the refinement of the X-ray data, and makes detailed comparisons of its bond parameters with those of its analogues impossible.

A perspective view of the structure of **6** (with the −3 axis drawn as a thin, horizontal line) is shown in Fig. 1, while crystal and refinement data and selected bond parameters are listed in Tables 1 and 2, respectively. This structural analogue of **2** is a dimer of two [P(μ-N^{t}Bu)$_2$P(^{t}BuN)$_2$]GeO moieties that are connected by a central (Ge–O)$_2$ rhombus. In Fig. 1 the chemically unique bonds are labeled 1–7, and this labeling scheme will be retained in the discussion of all molecular structures discussed below. The germanium-oxide bonds are 1.78(1) and 1.84(1) Å long and thus similar in length to the corresponding bonds in **2**, which are 1.809(4) and 1.825(4) Å long. The coordination sphere of the germanium atoms is completed by two sets of chemically inequivalent, but crystallographically-equivalent, nitrogen atoms. On chemical grounds the germanium-amido bonds (3) are expected to be considerably shorter than the donor bond (7), but here these bonds are rendered equivalent, both bond types appearing to be 1.936(12) Å long. This value is unrealistically long for the germanium–amido bonds (bond 3) and much too short for the donor bond (bond 7), c.f., the respective bond lengths of 1.887(6) Å and 2.369(6) Å in **2**.

The tin chalcogenides {[P(μ-N^{t}Bu)$_2$P(^{t}BuN)$_2$]SnE}$_2$, E = O (**7**), S (**8**), and Se (**9**), which were obtained as mono-toluene solvates, crystallize isotypically and ordered in the monoclinic space group *C*2/*m*. Crystal data and refinement parameters of these compounds are listed in Table 1, while selected bond lengths and angles appear in Table 2. These dimeric molecules have crystallographic 2/*m* symmetry, which is compatible with the molecular

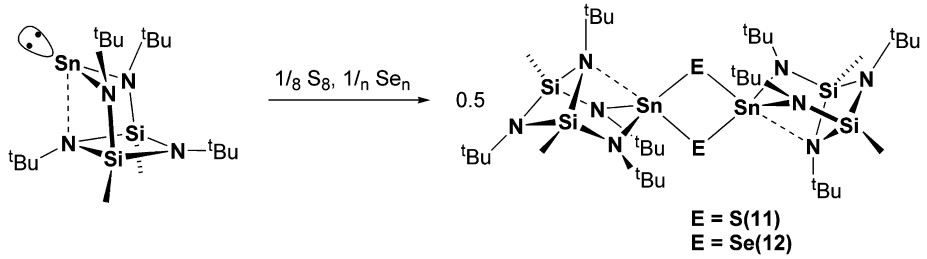

Scheme 5.

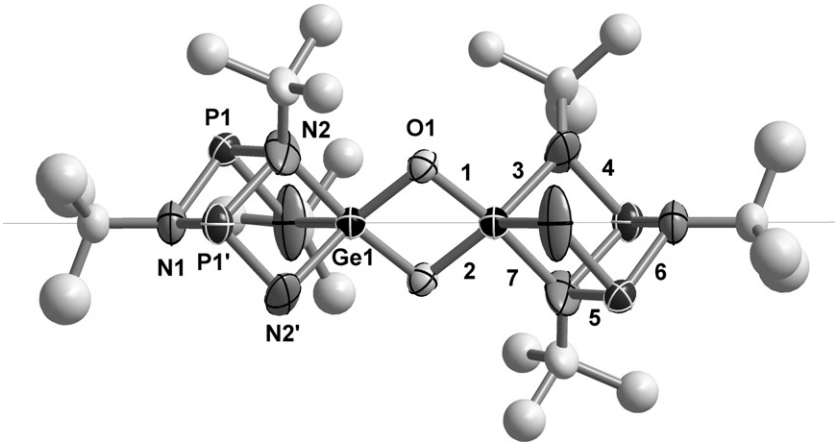

Fig. 1. Thermal–ellipsoid (35% probability) and partial labeling scheme of disordered **6.** The horizontal line represents the rotoinversion axis about which the molecule is disordered. The *tert*-butyl group on N2 and hydrogen atoms have been omitted to improve clarity.

Table 1
Crystal and refinement data for compounds **6**–**12**

	6	**7**	**8**	**9**	**10**	**11**	**12**
Chemical formula	$C_{32}H_{72}N_8O_2P_4Ge_2$	$C_{39}H_{80}N_8O_2P_4Sn_2$	$C_{39}H_{80}N_8P_4S_2Sn_2$	$C_{39}H_{80}N_8P_4Se_2Sn_2$	$C_{32}H_{72}N_8P_4S_4Sn_2$	$C_{36}H_{84}N_8S_2Si_4Sn_2$	$C_{36}H_{84}N_8Se_2Si_4Sn_2$
Formula weight	870.02	1054.37	1086.52	1180.32	1058.48	1042.95	1136.74
Space group	*Pa*−3 (No. 205)	*C*2/*m* (No. 12)	*C*2/*m* (No. 12)	*C*2/*m* (No. 12)	*Pbca* (No. 61)	$P2_1/n$ (No. 14)	$P2_1/n$ (No. 14)
T (°C)	24	−60	−80	−80	−80	20	20
a (Å)	16.4765(19)	24.0752(6)	23.7096(1)	23.6374(1)	15.961(2)	10.007(2)	9.976(2)
b (Å)	16.4765(19)	11.6275(3)	11.7950(1)	11.8163(1)	10.790(1)	17.086(6)	17.086(6)
c (Å)	16.4765(19)	9.8462(2)	9.8365(1)	9.9063(1)	27.207(3)	15.289(3)	15.417(3)
β (°)	–	112.883(1)	109.216(1)	108.541(1)	–	94.772	95.359(2)
V (Å^3)	4473.0(9)	2539.4(1)	2597.56(4)	2623.28(4)	4685(1)	2605(1)	2616.2(9)
Z	4	2	2	2	4	2	2
ρ_{calc} (g cm^{-3})	1.379	1.384	1.489	1.501	1.330	1.443	1.288
λ (Å)	0.710 73	0.710 73	0.710 73	0.710 73	0.710 73	0.710 73	0.710 73
μ (cm^{-1})	1.523	11.48	11.99	24.96	14.14	11.60	24.60
$R(F)$[a] $[I > 2\sigma(I)]$	0.038	0.0643	0.0305	0.0437	0.0459	0.0502	0.042
wR_2 (F^2)[b] (all data)	0.1847	0.0880	0.0976	0.0941	0.0968	0.046	0.042

[a] $R = \sum|F_o - F_c|/\sum|F_o|$.
[b] $R_w = \{[\sum w(F_o^2 - F_c)^2/[\sum w(F_o^2)^2]\}^{1/2}$; $w = 1/[\sigma^2(F_o)^2 + (xP)^2 + yP]$ where $P = (F_o^2 + 2F_c^2)/3$. For **11** and **12** $R_w = \{\sum|F_o - F_{cl}|^2/\sum|F_o|^2\}^{1/2}$; $w = 1/\sigma^2(F_o)$.

Table 2
Selected bond lengths (Å) and angles (°) for **6**–**12**

Bond type	**6**	**7**	**8**	**9**	**10**	**11**	**12**
Bond lengths							
M–N(3, avg.)	1.936(12), disordered	2.070(2)	2.084(3)	2.075(3)	2.098(3)	2.083(5)	2.107(4)
M–N(7)	1.936(12), disordered	2.327(3)	2.403(4)	2.420(4)	2.539(3)	2.487(5)	2.514(5)
M–E (2)	1.772(12)	1.997(3)	2.4157(12)	2.5420(6)	2.4146(10)	2.412(2)	2.5428(9)
M–E′ (1)	1.846(13)	2.014(3)	2.4601(12)	2.5930(6)	2.4542(10)	2.487(5)	2.6097(9)
P(Si)-μ-N(5, avg.)	1.938(12)	1.778(2)	1.791(3)	1.787(3)	1.746(4)	1.769(6)	1.778(5)
P(Si)-μ-N(6, avg.)	1.831(6)	1.728(2)	1.726(2)	1.723(3)	1.702(3)	1.743(6)	1.741(5)
P(Si)-μ-N(4, avg.)	1.945(12)	1.690(2)	1.691(3)	1.697(3)	1.668(3)	1.726(6)	1.729(5)
P═S					1.888(3)		
Bond angles							
N(amido)–M–N(amido)	84.8(5)	105.67(14)	105.6(2)	105.68(18)	105.08(12)	108.2(2)	108.3(2)
E–M–E′	84.6(6)	83.56(12)	90.75(4)	91.353(19)	90.33(3)	88.74(6)	89.45(3)
M–E–M′	95.4(6)	96.44(12)	89.25(4)	88.647(19)	89.67(3)	91.26(6)	90.55(3)
N(amido)–Sn–E	100.9(6)	111.28(8)	109.33(8)	109.29(9)	111.63(9)	108.3(2)	108.1(1)
N(amido)–Sn–E′	136.7(6)	121.37(8)	120.09(8)	119.85(9)	118.34(9)	120.2(2)	120.0(1)
N(imino)–Sn–E	172.2(5)	179.80(11)	173.37(9)	172.65(10)	174.16(8)	175.6(1)	177.3(1)

symmetry. The solid-state structure of the oxide $\{[P(\mu\text{-}^t BuN)_2P(^t BuN)_2]SnO\}_2$ (**7**), together with its partial atom and bond labeling schemes, is shown representatively for all three compounds in Fig. 2.

The coordination geometry about the tin atoms is intermediate between distorted trigonal-bipyramidal and distorted tetrahedral, plus an additional donor bond. Because of the variability of the donor bond lengths and their weakness (vide supra), we prefer to consider the Group 14 elements to be four-coordinate and having a fifth (weak) contact with one of the heterocyclic nitrogen atoms. The symmetrical tin amide bonds are rather insensitive to their environment, ranging from 2.070(2) Å for **7** to 2.098(3) Å for **10**, with a mean value of 2.085(3) Å. These bonds are somewhat shorter than those reported by Chivers et al. for Sn(IV)–N bonds in related Sn–N seco-heterocubes, which range from 2.116(4) to 2.157(5) Å [54–56]; they are also shorter than the Sn(IV)–N bonds in an amidinate tin sulfide [35], which were reported to be from 2.09(1) to 2.264(4) Å long.

The solid-state structure of **10** is shown in Fig. 3; it differs from those of **6**–**9** only in that one phosphorus atom of each ligand has been oxidized by sulfur. Pertinent crystal and refinement data are listed in Table 1, while Table 2 contains selected bond parameters. The isolated molecules of this compound are located on the inversion centers of the space group *Pbca*, and although the *trans* isomer **10a** can satisfy this site symmetry requirement, the *cis* isomer

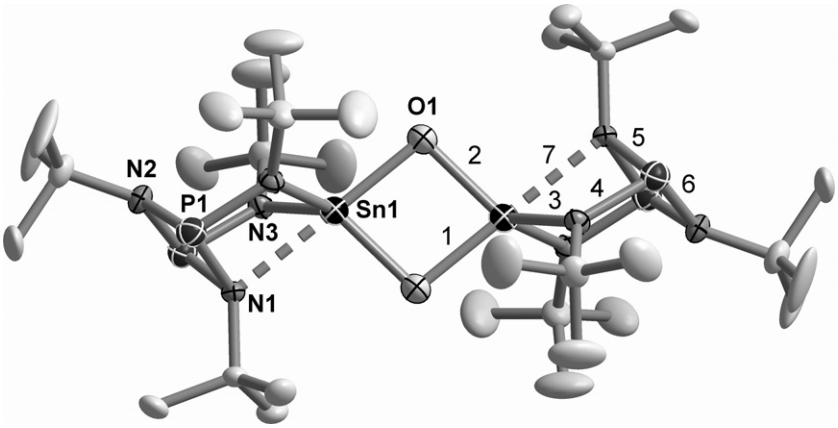

Fig. 2. Thermal–ellipsoid (35% probability) plot and partial labeling scheme of **7.** The sulfide (**8**) and selenide (**9**) analogues are isotypic. Hydrogen atoms have been omitted for clarity.

10b cannot. It is likely that the unit cells of the crystal contain both, disordered **10a** and disordered **10b**, because the structure refinement revealed that the P═S moieties are distributed over all four phosphorus atoms, leading to unrealistically short P═S bond lengths of 1.888(3) Å [61].

In contrast to the almost constant tin-amide bonds, the N → Sn donor interactions (7) are much more variable, falling into three distinct groups: namely, the short donor interaction (2.327(3) Å) of **7**, the intermediate-length contacts of 2.403(4) and 2.420(4) Å for **8** and **9**, respectively, and the rather long separation of 2.539(3) Å in **10**. Compounds **8** and **10** differ only in the presence of two P═S bond in **10**, and we therefore ascribe the significantly longer contact in **10** to the somewhat lower basicity of its cyclodiphosph(III/V)azane ring. The short contact of **7**, by contrast, is likely due to the much lower steric demands of the oxygen atoms. Although these donor interactions span the fairly wide range of 0.2 Å, the significance of this difference should not be overstressed. Based on X-ray structural data of related bis(*tert*-butylamido)cyclodiphosph(III)azanes the potential energy curve for the position of the central atom in these *seco*-heterocubic compounds must be fairly flat. This is demonstrated, for example, by the solid-state structure of $[P(\mu\text{-}N^tBu)_2P(^tBuN)_2]SiCl_2$ where the silicon atoms of two crystallographically-independent molecules make contacts of 2.168(3) and 2.423(3) Å, respectively, with the nitrogen atom of the $P(\mu\text{-}N^tBu)_2P$ heterocycle [62]. Because compounds **7**–**9** are isotypical, the P–N bond lengths of their cyclodiphosph(III)azane ligands are almost isometric. Expectedly, the presence of the pentavalent phosphorus atoms has shortened all P–N bonds of **10** compared to those in **7**–**9**, but due to the disorder a detailed discussion of their values would not be meaningful.

Like the cyclodiphosphazane-based tin chalcogenides **7**–**9**, the cyclodisilazane analogues **11** and **12** crystallize isotypically, but they do so with the same $\bar{1}$ site symmetry

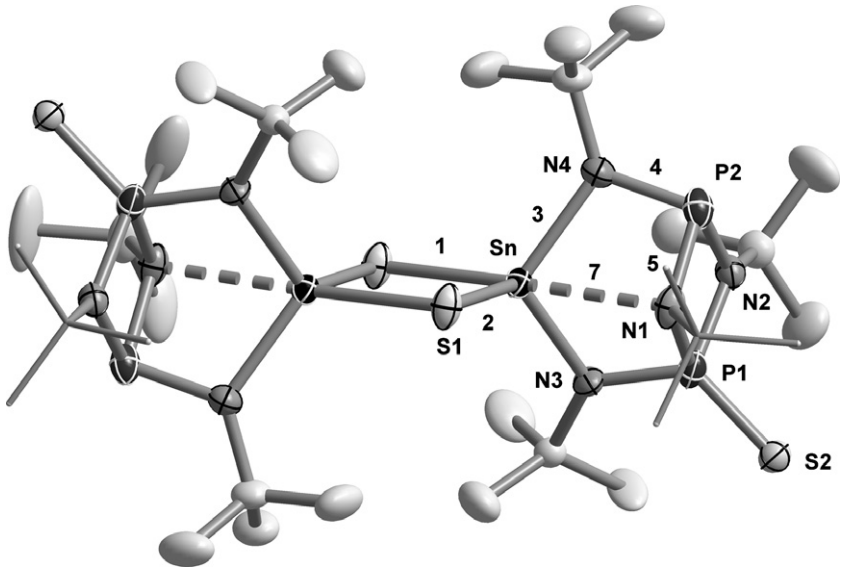

Fig. 3. Thermal–ellipsoid (50% probability) plot and partial labeling scheme of **10a**. Hydrogen atoms have been omitted and two of the *tert*-butyl groups are drawn in wire-format for improved clarity.

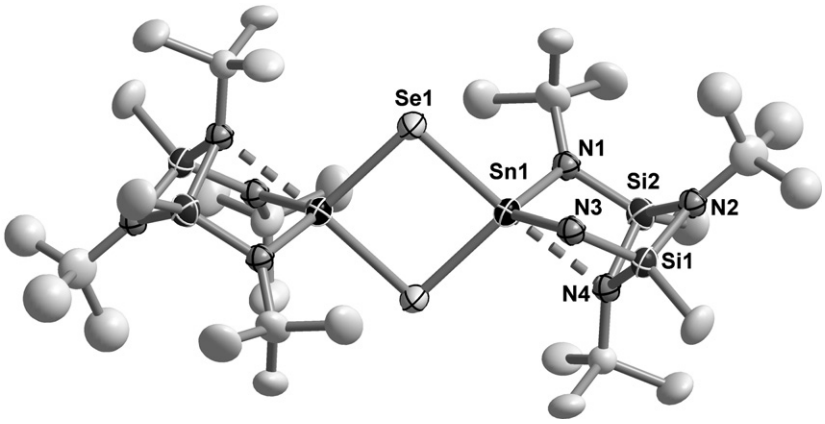

Fig. 4. Thermal–ellipsoid (50% probability) plot and partial labeling scheme of **12**; the sulfide analogue (**11**) is isotypic. The hydrogen atoms and the *tert*-butyl group on N3 have been omitted to improve clarity.

as **2**. Fig. 1 shows representatively the thermal–ellipsoid plot of the tin–selenide dimer **12**, and its partial labeling scheme. Pertinent crystal and refinement data for both compounds are listed in Table 1, while Table 2 contains selected bond parameters. The thermal–ellipsoid plot shows that these compounds are structural analogues of the germanium oxide dimer **2** and of the cyclodiphosphazane dimers **6**–**10**. Among the bond parameters of **11** and **12** only the Si1–N3 and Si2–N4 bonds (bond 4) are noticeably longer than the corresponding bonds of the cyclodiphosphazane-based analogues **8** and **9**, which is a typical increase seen for cyclodisilazane derivatives [59] (see Fig. 4).

Because of the central role of the Group 14 element-to-chalcogen bonds, their bond lengths, together with those of the previously reported compounds **2** and **3**, are listed in Table 3. All of these slightly rhombically-distorted, four-membered rings are located on special positions ($\bar{1}$ or 2/*m*) of their respective space groups, and they are therefore completely planar. To differentiate the bond parameters of the dimers having cyclodiphosphazane ligands from those having cyclodisilazane ligands, the values for the latter compounds are rendered in italic font. Two trends emerge from these data, namely the M–E bond lengths are essentially independent of the ligands, and the asymmetry of the M–E–M bonds, albeit small, increases on going from oxygen to selenium. The former observation demonstrates that neither the size nor the electronegativity differences between Si and P have any effect whatsoever on the structures of the central $(M–E)_2$ rings. The bond asymmetry, by contrast, is an indication of the increasing steric shielding of the Group 14 element by the larger chalcogenides and the concomitant inability of the metal(loid) to form two symmetrical M–E single bonds.

Thus, for example, the tin–oxide bonds of **7** are almost symmetrical at 1.997(3) and 2.014(3) Å, respectively; they are also equidistant (1.987(5), 2.001(5) Å) with those reported for a tin oxide dimer supported by octamethyldibenzotetraaza [14] annulene ligands (**F**, M = Sn, E = O) [34]. The tin–sulfur and tin–selenium bonds of **8** and **9**, however, are noticeably more asymmetrical, forming bond pairs of (2.4157(12), 2.4601(12) Å) and of (2.5420(6), 2.5930(6) Å), respectively. The average tin–sulfur bond lengths of **8**, **10** and **11** are quite similar to those observed for $\{[CyNC(Me)NCy]_2SnS\}_2$, where values of 2.434(2) and 2.476(2) Å were found [35]. The average tin–selenium bond lengths of **9** (2.568(6) Å) and of **12** (2.576(1) Å) are isometric with each other and only slightly longer than those found in the less sterically encumbered dimer $\{[(Me_3Si)_2N]_2SnSe\}_2$, whose Sn–Se bonds are 2.541(1) Å long [63].

Table 3
Bond lengths (Å) for selected Group 14 chalcogenide bonds of the title compounds and related chalcogenides

Bond type	**Ge–O**	**Ge–S** (terminal)	**Sn–O**	**Sn–S**	**Sn–Se**
Bond lengths (Å)	**6** 1.77(1), 1.85(1) **2** *1.825(5), 1.809(5)*	**3** *2.063(4)*	**7** 1.997(3), 2.014(3)	**8** 2.4157(12), 2.4601(12) **10** 2.4146(10), 2.4542(10) **11** *2.412(2), 2.487(2)*	**9** 2.5420(6), 2.5930(6) **12** *2.5428(9), 2.6097(9)*

2.3. Solution-phase NMR data

Just like the ^{1}H NMR spectra of the heterocarbenoids **4** and **5**, the ^{1}H NMR spectra of **6**–**12** display either three or two signals, depending on whether the *tert*-butylimino substituents of the $P(\mu\text{-}N^tBu)_2P$ heterocycle are diastereotopic (**N**) or isotopic (**O**), as shown in Chart 4. Characteristic for the first case are three signals (a, b and c) in a 2:1:1 ratio, for the *tert*-butylamido, and the two inequivalent *tert*-butylimino groups, respectively. The appearance of two signals of equal intensity is indicative of a fluxional behavior in the fast-exchange limit, with **N** presumably being the transition state of the equilibrating molecules. Both, the cyclodisilazane-based germanium oxide (**2**) and the germanium sulfide (**3**) exhibited asymmetric ground states, but

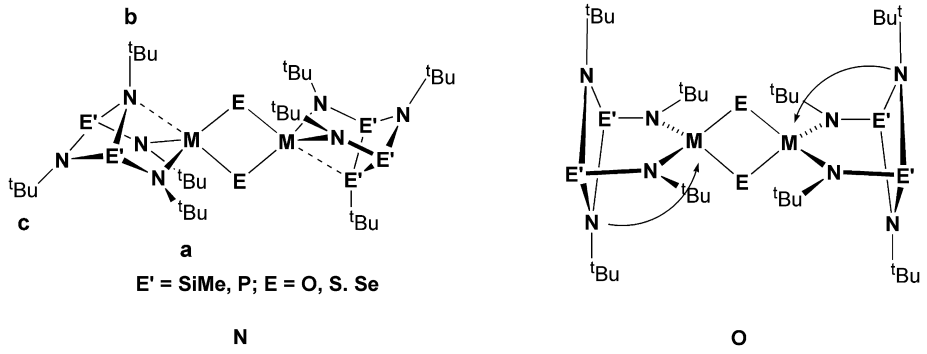

Chart 4.

upon heating to 307 K the signals of **3** coalesced, yielding an estimated activation energy of 16.3(2) kcal mol^{-1}. For the dimeric germanium oxide **2**, by contrast, the coalescence temperature of signals b and c was reportedly too high to be observed.

The very low solubility of **6**–**10** in common solvents made the recording of even ^1H NMR spectra, difficult. We were, however, able to confirm that compounds **6** and **9** have asymmetric ground-state solution structures that are analogous to the solid-state structures of all dimers, while **7**, **8**, and **10** are fluxional at room temperature.

Low solubility also prevented us from freezing out the ground-state structures for the fluxional dimers, and the compounds with low-symmetry ground states (**N**) showed no fluxionality up to readily attainable temperatures (80 °C).

The cyclodisilazane-based dimers **11** and **12** were more soluble, and thus much more amenable to solution phase NMR studies than their cyclodiphosphazane counterparts. Both compounds showed almost identical ^1H NMR spectra, with one singlet each for the *tert*-butylamido, *tert*-butylimino and methylsilyl groups. This pattern confirms that just like the cyclodiphosphazane derivatives **7**, **8**, and **10**, but unlike **2**, the cyclodisilazane analogues have fluxional solution structures (**O**) at room temperature.

3. Discussion

The heterocarbenoids of the heavier Group 14 elements are divalent compounds with electron deficient metal centers and strong tendencies to increase both the oxidation state and the coordination number of the central element. Above we showed that elemental chalcogens cleanly oxidize germylenes and stannylenes, supported by bis(*tert*-butylamido)cyclodiphosph(III)azane and -cyclodisilazane ligands, to the corresponding Group 14 chalcogenides. At room temperature these heterocarbenoids were rapidly oxidized with dioxygen, while the oxidations with sulfur and selenium were substantially slower, even at elevated temperatures. In one case excess sulfur partially oxidized the bis(*tert*-butylamido)cyclodiphosph(III)azane ligand as well, thereby furnishing a cyclodiphosph(III/V)azane derivative. Once oxidized, the Group 14 chalcogenides dimerized to the isolated final products, irrespective of whether the reactions were done at room temperature (**6**, **7**) or elevated temperatures (80 °C) as for **8**–**12**. These observations are an indication that the dimers are the thermodynamic products in these reactions and that the energy barriers to dimerization must be low.

The completely parallel results for the cyclodisilazane- and cyclodiphosphazane-based Group 14 carbenoids were not entirely unexpected, as previous studies had shown that these heterocyclic ligands have almost identical steric and electronic properties [59]. All seven oxidation products are dimeric with central, four-membered $(M–E)_2$ rings, and never were we able to isolate a monomeric germanium- or tin chalcogenide with a terminal double bond, as found in **3**.

Our extensive (but not comprehensive) data thus show that the bis(*tert*-butylamido)cyclodisilazanes and the isoelectronic bis(*tert*-butylamido)cyclodiphosphazanes are not particularly suitable for stabilizing the chalcogenides of their germanium and tin derivatives in monomeric form. The isolation of the first molecular compound with a terminal Ge=S bond (**3**) by Veith et al., was thus fortuitous and not the result of superior steric or electronic properties of the bis(*tert*-butylamido)cyclodisilazane ligand. Almost all of the ligands shown in Chart 2 are obviously better suited for stabilizing terminal Group 14 element chalcogenides than the heterocyclic diamines **L** and **M**. It is, of course, unfortunate that we failed to synthesize the bis(*tert*-butylamido)cyclodiphosphazane analogue of **3**, as this would have further supported the notion that the unique combination of germanium and the larger chalcogen, sulfur, is responsible for the stability of the terminal Ge=S bond in **3**.

Terminal Group 14 chalcogenides have traditionally been labeled "base-stabilized" or "kinetically-stabilized" depending on whether they were considered thermodynamic or kinetic products, respectively. Thus, terminal Group 14 chalcogenides in which the Group 14 element bears two very bulky aryl groups (**I**, Chart 2) are commonly called "kinetically-stabilized", while those in which the Group 14 element bears *N*-donor ligands and has

higher coordination numbers (4 or 5) are called "base-stabilized" Group 14 chalcogenides (**P**). As early as 1998, Kuchta and Parkin had asserted, that "it is imprudent to assume that the isolation of a particular terminal chalcogenido complex has either a kinetic or thermodynamic origin", and thus apparently questioned for the first time the validity of this division [64].

A monomeric Group 14 chalcogenide with a terminal M=E bond may be said to be a kinetic product if it converts to the dimer at elevated temperatures, as shown in Scheme 6. Applying this standard definition of kinetic stabilization, we were able to find merely one example of a kinetically-stabilized Group 14 chalcogenide in the literature [42], and even in that case the evidence is circumstantial.

Sufficiently precise theoretical calculations may also provide a good indication of the bond energetics in Group 14 chalcogenides and the relative tendencies of terminal chalcogenides to dimerize or to oligomerize. Using computational studies at the B3LYP/TZ(d,p) level Tokitoh et al. investigated the bond energies for the σ- and π-bonds in formaldehyde and its homologues of the type $H_2M{=}E$, where M is a Group 14 element and E is a chalcogen [49]. A partial listing of the σ- and π-bond energies for the germanium and tin homologues, obtained from this study, is given in Table 4. While the π-bond in formaldehyde is actually stronger (95.3 kcal mol^{-1}) than the σ bond (93.6 kcal mol^{-1}), it is substantially weaker for all germanium- and tin chalcogenides, and usually less than half as strong.

These data indicate that formaldehyde's heavier homologues have a strong thermodynamic preference for the formation of single bonds over double bonds, and that they are therefore thermodynamically unstable with respect to dimerization or oligomerization. This tendency is strongest for the oxides and weaker for the heavier chalcogens, all of which have approximately equal tendencies for single-bond formation over double-bond formation.

Data, like those in Table 4, bias the reader into believing that in the face of this seemingly overwhelming thermodynamic driving force for dimerization (or oligomerization), monomeric Group 14 chalcogenides must be kinetic products. For the sterically much more encumbered molecules shown in Chart 2 and in this work, however, the Gibbs free energies of dimerization are likely considerably less negative than suggested by the data in Table 4, and often they are obviously positive. The importance of steric bulk in

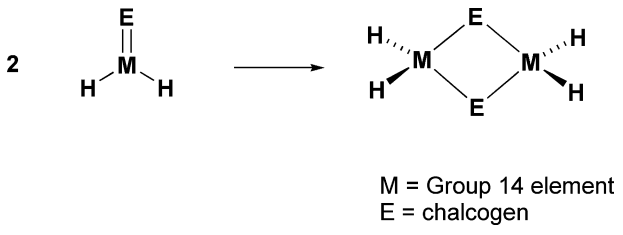

Scheme 6.

Table 4
M=E bond energies (kcal) for $H_2M{=}E$ homologues, (M = Ge, Sn; E = chalcogen), based on data from reference [49]

	O	S	Se	Te
Ge				
σ-Bond energy	101.5	74.1	67.8	59.1
π-Bond energy	45.9	41.1	36.3	30.3
(as % of σ-bond energy)	(45.2)	(55.5)	(53.5)	(51.3)
Sn				
σ-bond energy	94.8	69.3	64.3	56.4
π-bond energy	32.8	33.5	30.6	26.3
(as % of σ-bond energy)	(34.6)	(48.3)	(47.6)	(46.6)

the degree of aggregation of Group 14 chalcogenides is impressively demonstrated by comparing formaldehyde with acetone. Thus, while acetone is stable to head-to-tail dimerization, formaldehyde is unstable to trimerization by ca. 10 kcal per mole of formaldehyde [65].

Even with this reduction in dimerization energies because of substituent effects it may be expected that the overall thermodynamic trends will remain the same as for the formaldehyde homologues. Namely, for any given class of homologous Group 14 chalcogenides the oxides will exhibit the greatest tendency to dimerize, while the heavier chalcogenides will have lesser tendencies to do so [66]. The data in Table 4 also predict germanium chalcogenides to be less prone to dimerize than the tin analogues, and this trend is indeed observed empirically.

Double bonds between Group 14 and Group 16 elements differ from conventional double bonds in that the coordination number of the chalcogen is invariably one, while that of the Group 14 element may vary from three and five [50]. Steric stabilization of Group 14 chalcogenides is therefore mainly imparted by both the number and the nature of the substituents on the Group 14 element. Steric protection against dimerization may also be provided by the size of the chalcogen, with large chalcogens coordinated to small Group 14 elements being particularly effective in stabilizing monomeric structures.

This is shown in Fig. 5 where Ge=E moieties (E = O, S, Se, Te) obtained from various solid-state structure determinations are depicted [67]. It is obvious that the largest chalcogen, tellurium, effectively blocks a much larger portion of the germanium atom's surface than oxygen, thereby hindering the formation of additional bonds. These size differences become even more important in sterically congested Group 14 chalcogenides, such as those shown in Chart 2.

As Table 4 shows, formaldehyde and its heavier homologues are inherently unstable to dimerization or oligomerization, and this instability is a factor of both the Group 14 element and the chalcogen. While high-level calculations of real Group 14 chalcogenides, such as those shown in Chart 2, are not available, it is clear from empirical studies that their thermodynamic driving force to dimerize is significantly reduced by the steric and electronic factors imparted by the substituents. Thus, the free energies for the dimer-

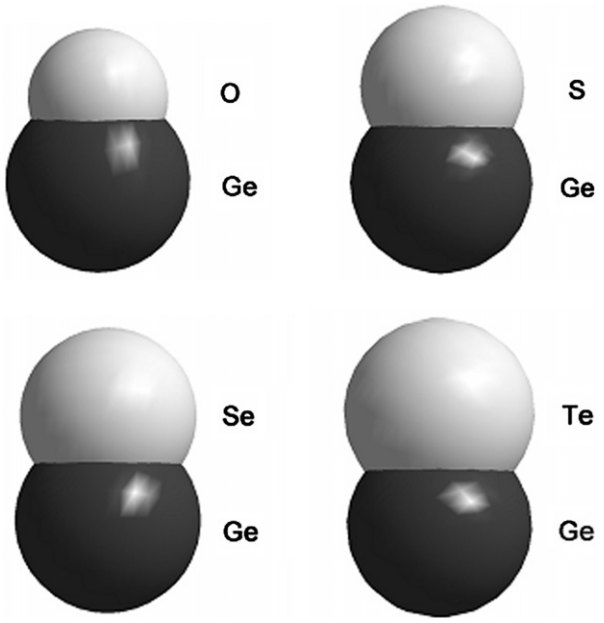

Fig. 5. Space-filling drawings of germanium chalcogenide moieties, demonstrating the substantially greater steric demands of the heavier chalcogens.

ization of "real" Group 14 chalcogenides are often very close to zero.

For example, dimeric **2** and monomeric **3** differ solely in the chalcogen. Here obviously the germanium sulfide **3** is sufficiently sterically encumbered to remain monomeric, while the oxide, whose Ge=O moiety is inherently more prone to dimerize, is still insufficiently sterically-protected and therefore dimerizes. Similar observations were made by Chivers and associates for the *seco*-heterocubic compounds of type **K** [55], which are close structural relatives of the title compounds. The sulfide derivative of **K** was isolated in dimeric form, while the telluride was monomeric with a terminal Sn=Te bond. The selenide, by contrast, existed in solution as an equilibrium mixture of monomers and dimers.

The tin–sulfide and the tin–selenide derivatives were synthesized by the relatively short (30 min) interaction of tin(II) complex and the appropriate chalcogen at low temperature (40 °C). The terminal tin–telluride, which was synthesized by heating the tin(II) compound with tellurium for 16 h at 100 °C, is obviously a thermodynamic product. Because these compounds, just like **2** and **3**, differ only in the chalcogen, their degree of aggregation is controlled by the bond enthalpies of the M=E and M–E bonds and the size differences of the chalcogens.

Even more subtle factors have been observed to control the dimerization of related Group 14 chalcogenides. For example, Richeson et al. isolated the *tert*-butyl-substituted amidinato-tin sulfide [CyNC(^{t}Bu)NCy]SnS (Cy = cyclohexyl) in monomeric form, while the methyl-substituted analogue{CyNC(Me)NCy]SnS}$_2$ was dimeric [35], suggestive of very delicate steric and/or electronic factors.

We thus conclude that the chalcogenides of Group 14 heterocarbenoids and related divalent Group 14 compounds bearing N-donor ligands are thermodynamic products. We do, however, believe that the label "base stabilized" is an over-interpretation of the available data. The term "base stabilization" is usually meant to imply that the coordination of a Lewis base to an M=E bond stabilizes the buildup of positive charge on the Group 14 electronically, as shown in **P** (Chart 5), thereby preventing dimerization. Such donor interactions, however, are seen in all of the title compounds, in addition to **2** and **3**, yet only the germanium sulfide **3** was isolated with a terminal Ge=S bond. The much shorter distance for this donor interaction in **3** compared to those in its structural analogues is, in our opinion, the *result of* and *not the reason for* its monomeric structure.

If Lewis-base stabilization were indeed important for stabilizing terminal Group chalcogenide bonds it should be most developed in the more polar Ge=O, rather than the less polar Ge=S, bond. A more likely reason for the unique reluctance of **3** in this class of compounds to dimerize is the precipitous drop in the relative magnitude of the π-bond energy on going from germanium sulfide to germanium oxide. If this is indeed so, then the selenide and the telluride analogues, which have similar bond energies as the sulfide but feature even larger chalcogens, should also be monomeric. It is not difficult to predict that this will likely be the case.

The label "kinetically-stabilized", terminal chalcogenide bond is used almost exclusively in conjunction with the "heavy ketones", i.e., diarylelement chalcogenides of Group 14 (Chart 6), although in principle it should be applicable to any type of terminal Group 14 chalcogenide. If one were to find kinetically-stabilized terminal Group 14 chalcogenides, then it would certainly have to be among this class of compounds. We, therefore, scrutinized all available data on "heavy ketones" for definitive evidence of kinetic stabilization [42–53], namely the conversion of monomeric to dimeric chalcogenides at elevated temperatures. But among the approximately one dozen of such terminal chalcogenides described in the literature we found circumstantial evidence of kinetic stabilization in only one case [53]. There was, however, clear experimental evidence that most isolated "heavy ketones" are really thermodynamic products.

Thus, we are told that compounds **Ib, Ic**, and **Id** were synthesized by treating the germylene (Tip)(Tbt)Ge at

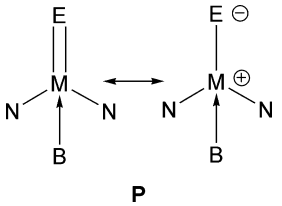

P

Chart 5.

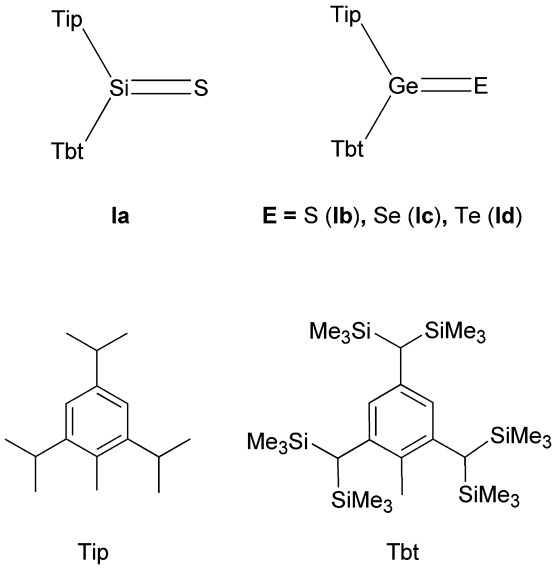

Chart 6.

90 °C with elemental chalcogen for 7 (S, Se) [51] and 25 (Te) days [47], respectively. The germanethione **Ib**, which melts at 163–165 °C without decomposition, was reportedly recovered unchanged even after it had been kept at 160 °C in a sealed tube for 3 days [51]! The authors describe the silanethione **Ia** as thermally stable to its melting point of 185–189 °C and reluctant to dimerize upon refluxing in hexane for 2 h [49]. These observations are textbook cases of thermodynamic stability and leave little doubt that the isolated "kinetically-stabilized" Group 14 chalcogenides are really thermodynamic products.

In summary, the heavier homologues of formaldehyde have an inherent thermodynamic tendency to dimerize or oligomerize. For any given Group 14 element this tendency is largest for oxides and significantly smaller for the heavier chalcogenides, which, as a group, have similar tendencies to dimerize. This thermodynamic driving force is reduced, or even negated, by the ligands on the Group 14 elements and by the steric bulk of the chalcogen atoms. As a consequence, numerous molecular Group 14 chalcogenides, featuring terminal M=E double bonds, are now known. It is not yet possible to ascertain how much of this stabilization is due to the inherent energetics of the M=E moieties, the steric and electronic factors exerted by the ancillary ligands, or the size of the chalcogen. It does appear, however, that most if not all, currently known Group 14 chalcogenides are thermodynamic, rather than kinetic, products.

4. Conclusion

Bis(*tert*-butylamido)cyclodiphosphazanes and -cyclodisilazanes of Group 14 elements are structurally interesting heterocarbenoids, that are characterized by high reactivity and a potentially rich coordination chemistry. Despite their electron-deficiency, the two-coordinate, divalent Group 14 elements are readily oxidized by elemental chalcogens to form dimeric polycycles with central $(M–E)_2$ rings. The reluctance of these compounds to exhibit monomeric structures with terminal M=E double bonds, as had been observed for the germanium sulfide (**3**) of one of these ligands, is due to the thermodynamic unfavorability of such structures and the kinetic labilities of the monomers to dimerization.

All terminal Group 14 chalcogenide, including those labeled "kinetically-stabilized", should be considered thermodynamic products, unless a good case for kinetic stabilization can be made. While the label "base-stabilized" double bond is less troublesome, it is, in our opinion, an over-interpretation of the available data. The descriptive and unambiguous terms "terminal Group 14 chalcogenides" and "bridging Group 14 chalcogenides" would therefore seem superior to distinguish between the two structural variants of Group 14 chalcogenides.

5. Experimental

5.1. General considerations

All operations were performed under an atmosphere of argon or prepurified nitrogen on conventional Schlenk lines. The hydrocarbon or ethereal solvents were predried over molecular sieves or CaH_2 and distilled under a nitrogen atmosphere from sodium or potassium benzophenone ketyl immediately before use. Anhydrous stannous chloride [68], and *cis*-$[P(\mu\text{-}^t BuN)_2P(^t BuNLi \cdot THF)_2]$ [59] were synthesized according to previously published procedures. $GeCl_2 \cdot$ dioxane was purchased from Gelest and used as received. Mass spectra were recorded on a VG Micromass 7070E-HF double-focusing spectrometer, in the FAB mode, using an MNBA (*meta*-nitrobenzyl alcohol) matrix, or in the chemical ionization mode, using methane as the reacting gas. NMR spectra were recorded on Varian VXR-300 and Bruker Avance 500 spectrometers. The ^1H, ^{13}C and ^{31}P NMR spectra are referenced relative to C_6D_5H (7.15 ppm), C_6H_6 (128.0 ppm), and external $P(OEt)_3$ (137.0 ppm), respectively, with shifts to higher frequency (lower field) given a more positive value. Melting points were recorded on a Mel-Temp melting point apparatus; they are uncorrected. E&R Microanalytical Laboratory, Inc., Parsippany, NJ, performed the elemental analyses. Mass spectral data were recorded on a VG 7070E-HF instrument at the Mass Spectral Service Laboratory of Montana State University, Bozeman, MT.

6. Syntheses

6.1. $[P(\mu\text{-}N^tBu)_2P(^tBuN)_2]Ge$, **4**

A solution of germanium dichloride · dioxane (0.61 g, 2.6 mmol) in THF (5 mL) was cooled to 0 °C and treated dropwise with $[P(\mu\text{-}^t BuN)_2P(^t BuNLi \cdot THF)_2]$ (1.4 g, 2.8 mmol), dissolved in 20 mL of THF. The reaction mix-

ture was then refluxed for 14 h, allowed to cool, filtered through a medium-porosity frit and concentrated *in vacuo* to ca. 5 mL. After the solution had been stored at −21 °C for several days, 0.98 g (88%) of a yellow, amorphous solid precipitated.

M.p..: 188–194 °C. ^{1}H NMR (300 MHz, benzene-d_6, 26 °C) $\delta = 1.43$ (s, 18H), 1.41 (s, 18H). ^{13}C{^{1}H} NMR (75 MHz, benzene-d_6, 26 °C) $\delta = 57.51$ (s), 55.87 (s), 33.34 (d, $J = 8.6$ Hz), 27.61 (t, $J = 6.7$ Hz). ^{31}P{^{1}H} NMR (121 MHz, benzene-d_6, 26 °C) $\delta = 118.97$ (s). Anal. Calc. for $C_{16}H_{36}GeN_4P_2$: C, 45.86; H, 8.66; N, 13.37. Found: C, 45.95; H, 8.86; N, 13.18%.

6.2. [P(μ-N^{t}Bu)$_2$P(^{t}BuN)$_2$]Sn, **5**

A solution of anhydrous $SnCl_2$ (0.74 g, 3.9 mmol) in 5 mL of THF was cooled to 0 °C and treated dropwise with a solution of [P(μ-^{t}BuN)$_2$P(^{t}BuNLi · THF)$_2$] (1.97 g, 3.91 mmol), dissolved in 20 mL of toluene. After a few drops of the dilithium salt had been added, the reaction mixture turned bright yellow and a precipitate of lithium chloride formed. The solution was stirred at room temperature for 24 h, and the solvents were removed in vacuo. The solid residue was redissolved in 15 mL of hexanes and the filtrate was evaporated to dryness, resulting in 1.57 g (3.38 mmol) of a bright-yellow, semi-crystalline solid. Overall yield: 88.5%. M.p.: 86 °C. ^{1}H NMR (300 MHz, benzene-d_6, 26 °C): δ 1.436 (s, 18H), 1.396 (s, 18H). ^{13}C{^{1}H} NMR (75 MHz, benzene-d_6, 26 °C): δ 54.16 (d, $J = 15$ Hz), 53.74 (t, $J = 38$ Hz), 34.68 (d, $J = 38$ Hz), 28.04 (t, $J = 27$ Hz). ^{31}P{^{1}H} NMR (121 MHz, benzene-d_6, 26 °C): δ 196.65 (s). Anal. Calc. for $C_{16}H_{36}N_4P_2Sn$: C, 41.31; H, 7.80; N, 12.05. Found: C, 41.35; H, 7.96; N, 11.64%.

6.3. {[P(μ-^{t}BuN)$_2$P(^{t}BuN)$_2$]GeO}$_2$, **6**

A toluene-solution of **4** (0.42 g, 1.0 mmol) was saturated with O_2 by continuously bubbling the gas through the solution for 10 min. As the yellow color of the solution faded, a colorless solid precipitated. The flask was closed and stored at 2 °C for several hours while a colorless solid formed. Removal of the supernatant yielded 0.32 g (0.73 mmol) of a colorless, crystalline solid (73%). Colorless, octahedral crystals, suitable for X-ray diffraction studies, were grown from a warm (50 °C) toluene solution.

M.p.: 226 °C (dec.). ^{1}H NMR (500 MHz, benzene-d_6, 21 °C) $\delta = 1.75$ (s, 18H), 1.67 (s, 9H), 1.33 (s, 9H). ^{31}P{^{1}H} NMR (202 MHz, benzene-d_6, 21 °C) $\delta = 162.8$ (s). Anal. Calc. for $C_{32}H_{72}Ge_2N_8O_2P_4$: C, 44.17; H, 8.34; N, 12.88. Found: C, 43.75; H, 8.10; N, 12.81%.

6.4. {[P(μ-^{t}BuN)$_2$P(^{t}BuN)$_2$]SnO}$_2$ · CH$_3$C$_6$H$_5$, **7**

A solution of **5** (0.426 g, 0.916 mmol) in toluene (50 mL), was saturated with O_2, delivered via pipet from a tank of highly-pure oxygen. The yellow color of the solution was discharged almost immediately. The solution was stirred for 6 h, then concentrated in volume, and cooled to −18 °C to afford 0.444 g of colorless, needle-shaped crystals. Yield: 92%. M.p.: 254–256 °C. ^{1}H NMR (300 MHz, benzene-d_6, 26 °C): δ 1.655 (s, 36H) 1.509 (s, 36H). ^{13}C{^{1}H} NMR (75 MHz, benzene-d_6, 26 °C): δ 55.39 (t, $J = 30$ Hz), 54.60 (d, $J = 31$ Hz), 35.15 (t, $J = 22$ Hz), 30.23 (m). ^{31}P{^{1}H} NMR (121 MHz, benzene-d_6, 26 °C): δ 151.44 (s). Mass spectrum (FAB, MNBA): m/z 965.3 = [M+H]$^+$. Anal. Calc. for $C_{39}H_{80}N_8O_2P_4Sn_2$: C, 44.42; H, 7.65; N, 10.63. Found: C, 44.27; H, 7.41; N, 10.46%.

6.5. {[P(μ-^{t}BuN)$_2$P(^{t}BuN)$_2$]SnS}$_2$ · CH$_3$C$_6$H$_5$, **8**

A mixture of **5** (0.524 g, 1.13 mmol) and elemental sulfur (0.036 g, 1.13 mmol) was heated in toluene (100 mL) at 80 °C for 48 h. The solution was allowed to cool to RT, concentrated to 50 mL and kept at −18 °C for 1 day to afford extremely insoluble, plate-like, yellow crystals. Yield: 0.54 g, 88%. M.p.: 238 °C. ^{1}H NMR (300 MHz, benzene-d_6, 26 °C): δ 1.47 (s, 36H), 1.39 (s, 36H). ^{13}C{^{1}H} NMR (75 MHz, benzene-d_6, 26 °C): δ 54.98 (m), 53.45 (m), 33.31 (m), 29.67 (m). ^{31}P{^{1}H} NMR (121 MHz, benzene-d_6, 26 °C): δ 91.23 (s). Mass spectrum (FAB, MNBA): m/z 994.8 = [M+H]$^+$. Anal. Calc. for $C_{39}H_{80}N_8P_4S_2Sn_2$: C, 43.11; H, 7.42; N, 10.31. Found: C, 43.29; H, 7.21; N, 10.16%.

6.6. {[P(μ-^{t}BuN)$_2$P(^{t}BuN)$_2$]SnSe}$_2$ · CH$_3$C$_6$H$_5$, **9**

In a manner identical to that used for the synthesis of **8**, **5** (0.392 g, 0.841 mmol) and grey selenium (0.066 g, 0.84 mmol) were allowed to react in 100 mL of toluene for 48 h.

Yield: 0.41 g, 82%. M.p.: 236–238 °C. ^{1}H NMR (300 MHz, benzene-d_6, 26 °C): δ 1.653 (s, 36H), 1.117 (s, 18H), 1.083 (s, 6H), 1.078 (s, 12H). ^{13}C{^{1}H} NMR (75 MHz, benzene-d_6, 26 °C): δ 54.98 (m), 53.45 (m), 32.50 (d, $J = 26$ Hz), 31.73 (t, $J = 17$ Hz), 31.06 (t, $J = 20$ Hz). ^{31}P{^{1}H} NMR (121 MHz, benzene-d_6, 26 °C): δ 81.62 (s). Anal. Calc. for $C_{39}H_{80}N_8P_4Se_2Sn_2$: C, 39.69; H, 6.83; N, 9.49. Found: C, 39.84; H, 6.81; N, 9.19%.

6.7. {[(SP(μ-^{t}BuN)$_2$P)(^{t}BuN)$_2$]SnS}$_2$, **10**

In a manner identical to that used for the synthesis of **8**, **5** (0.753 g, 1.62 mmol) and elemental sulfur (0.104 g, 3.45 mmol) were allowed to react in 100 mL of toluene. Light-yellow plates (0.67 g, 78%) were isolated upon refrigeration of the solution at −18 °C for 2 days. M.p.: 236–238 °C. ^{1}H NMR (300 MHz, benzene-d_6, 26 °C): δ 1.96 (s, 9H), 1.62 (s, 9H), 1.584 (s, 18H), (incomplete). ^{13}C{^{1}H} NMR (75 MHz, benzene-d_6, 26 °C): δ 35.16 (m), 34.75 (m), 30.24 (m). ^{31}P{^{1}H} NMR (121 MHz, benzene-d_6, 26 °C): δ 92.72 (d), 62.25 (d). Mass spectrum (FAB, MNBA): m/z 1061.1871 = [M+H]$^+$. Anal. Calc. for

$C_{32}H_{72}N_8P_4S_4Sn_2$: C, 36.31; H, 6.86; N, 10.59. Found: C, 36.32; H, 6.85; N, 10.41%.

6.8. {[MeSi(μ-^{t}BuN)$_2$SiMe(^{t}BuN)$_2$]SnS}$_2$, 11

A sample of [MeSi(μ-^{t}BuN)$_2$SiMe(^{t}BuN)$_2$]Sn (0.129 g, 0.264 mmol) and excess sulfur (0.729 g, 22.7 mmol) were dissolved in 25 mL of toluene and stirred at 70 °C for 24 h. The reaction mixture was then filtered warm through a medium-porosity frit, and the yellow solution was kept at 2 °C until crystals had formed. Yield: 0.122 g (88.6%) of rhombic crystals.

M.p.: 302 °C. ^{1}H NMR (300 MHz, benzene-d_6, 25 °C): $\delta = 1.814$ (s, 18H; N^{t}Bu), 1.375 (s, 18H; N^{t}Bu), 0.665 (s, 6H; SiMe). ^{13}C{^{1}H} NMR (75 MHz, benzene-d_6, 25 °C): $\delta = 55.0$ (s, NCMe$_3$), 52.5 (s, NCMe$_3$), 36.3 (s, NC*Me*$_3$), 33.7 (s, NC*Me*$_3$), 7.0 (s, SiMe). Mass spectrum (FAB, MNBA): *m*/*z* (%) 1038.49 (0.3), 1039.49 (0.5), 1040.70 (0.8), 1041.72 (0.8), 1042.71 (1.0), 1043.71 (0.9), 1044.71 (1.0), 1045.69 (0.6), 1046.71 (0.5), 1047.71 (0.2), 1048.72 (0.3). Anal. Calc. for $C_{36}H_{84}N_8Si_4Sn_2S_2$: C, 41.46; H, 8.12; N, 10.74. Found: C, 41.07; H, 8.21; N, 10.12%.

6.9. {[MeSi(μ-^{t}BuN)$_2$SiMe(^{t}BuN)$_2$]SnSe}$_2$, 12

In a manner identical to that used for the synthesis of **11**, [MeSi(μ-^{t}BuN)$_2$SiMe(^{t}BuN)$_2$]Sn (0.22 g, 45 mmol) and grey selenium (0.042 g, 0.53 mmol) were allowed to react in 25 mL of toluene. The solution was kept at 70 °C for 24 h, filtered through a medium-porosity frit and stored at 2 °C. Yield: 0.209 g, (81.8%) of colorless, rhombic crystals.

M.p.: 304 °C. ^{1}H NMR (300 MHz, benzene-d_6, 25 °C): $\delta = 1.847$ (s, 18H; N^{t}Bu), 1.339 (s, 18H; N^{t}Bu), 0.654 (s, 6H; SiMe). ^{13}C{^{1}H} NMR (75 MHz, benzene-d_6, 25 °C): $\delta = 55.5$ (s, NCMe$_3$), 52.3 (s, NCMe$_3$), 36.6 (s, NC*Me*$_3$), 33.9 (s, NC*Me*$_3$), 7.35 (s, SiMe). Mass spectrum (FAB, MNBA): *m*/*z* (%) 1135.86 (4.0), 1136.85 (4.6), 1137.86 (4.1), 1138.85 (4.1), 1139.85 (3.2). Anal. Calc. for $C_{36}H_{84}N_8Se_2Si_4Sn_2$: C, 38.04; H, 7.45; N, 9.86. Found: C, 38.39; H, 7.61; N, 9.52%.

7. X-ray crystallography

7.1. Compounds 6–10

All crystals were grown from supersaturated solutions at the indicated temperatures. Suitable, single crystals were coated with oil, affixed to a glass capillary, and centered on the diffractometer in a stream of cold nitrogen. Reflection intensities were collected with a Bruker SMART CCD diffractometer, equipped with an LT-2 low-temperature apparatus, operating at 193 K (213 K for **7**, and 297 K for **6**). Data were measured using ω scans of 0.3° per frame for 30 s until a complete hemisphere had been collected. The first 50 frames were recollected at the end of the data collection to monitor for decay. Cell parameters were retrieved using SMART [69] software and refined with SAINT [70] on all observed reflections. Data were reduced with SAINT, which corrects for Lorentz and polarization effects and decay. An empirical absorption correction was applied with SADABS [71]. The structures were solved by direct methods with the SHELXS-90 [72] program and refined by full-matrix least squares methods on F^2 with SHELXL-97 [73], incorporated in SHELXTL Version 5.10 [74].

7.2. Compounds 11 and 12

Crystal data were collected at 293 K on an Enraf-Nonius CAD 4 diffractometer using graphite-monochromated Mo Kα radiation ($\lambda = 0.71069$ Å). The structures were solved with Patterson methods and refined by full-matrix least squares against *F*. Data reductions, structure solutions and least-squares refinements were performed with the software programs NRCVAX DATRDR, NRCVAX SOLVER and NRCVAX LSTSQ [75].

Acknowledgement

We thank the University of North Dakota and ND EPSCoR for financial support.

Appendix A. Supplementary material

CCDC 671134, 671135, 671136, 671137, 671138, 671139 and 671140 contain the supplementary crystallographic data for **6**, **7**, **8**, **9**, **10**, **11** and **12**. These data can be obtained free of charge from The Cambridge Crystallographic Data Centre via www.ccdc.cam.ac.uk/data_request/cif. Supplementary data associated with this article can be found, in the online version, at doi:10.1016/j.jorganchem.2007.12.031.

References

[1] A.J. Arduengo III, Acc. Chem. Res. 32 (1999) 913–921.
[2] D. Bourissou, O. Guerret, F.P. Gabbaï, G. Bertrand, Chem. Rev. 100 (2000) 39–92.
[3] W.A. Herrmann, Angew. Chem., Int. Ed. 41 (2002) 1290–1309.
[4] G. Bertrand (Ed.), Carbene Chemistry: From Fleeting Intermediates to Powerful Reagents, Marcel Dekker, New York, 2002.
[5] H.-W. Wanzlick, E. Schikora, Chem. Ber. 94 (1961) 150–154.
[6] H.-W. Wanzlick, H.-J. Schönherr, Angew. Chem., Int. Ed. Engl. 7 (1968) 141–142.
[7] K. Öfele, J. Organomet. Chem. 12 (1968) P42–P43.
[8] A.J. Arduengo III, R.L. Harlow, M. Kline, J. Am. Chem. Soc. 113 (1991) 361–363.
[9] A.J. Arduengo III, M. Kline, J.C. Calabrese, F. Davidson, J. Am. Chem. Soc. 113 (1991) 9704–9705.
[10] E. Despagnet-Ayoub, R.H. Grubbs, J. Am. Chem. Soc. 126 (2004) 10198–10199.
[11] T.D. Forster, K.E. Krahulic, H.M. Tuononen, R. McDonald, M. Parvez, R. Roesler, Angew. Chem., Int. Ed. 45 (2006) 6356–6359.
[12] D.S. McGuiness, K.J. Cavell, Organometallics 19 (2000) 741–748.

[13] W.A. Herrmann, C.-P. Reisinger, M. Spiegler, J. Organomet. Chem. 557 (1998) 93–96.
[14] C. Zhang, J. Huang, M.L. Trudell, S.P. Nolan, J. Organomet. Chem. 64 (1999) 3804–3805.
[15] W.A. Herrmann, J. Schwarz, M.G. Gardines, Organometallics 18 (1999) 4082–4089.
[16] T. Weskamp, W.C. Schattenmann, M. Spiegler, W.A. Herrmann, Angew. Chem., Int. Ed. Engl. 37 (1998) 2490–2493.
[17] M. Scholl, T.M. Trnka, J.P. Morgan, R.H. Grubbs, Tetrahedron Lett. 40 (1999) 2247–2250.
[18] J. Huang, H.Z. Schanz, E.D. Stevens, S.P. Nolan, Organometallics 18 (1999) 3760–3763.
[19] M. Mühlhofer, T. Strassner, W.A. Herrmann, Angew. Chem., Int. Ed. Engl. 41 (2002) 1745–1747.
[20] D.J. Cardin, B. Cetinkaya, M.J. Doyle, M.F. Lappert, Chem. Soc. Rev. 2 (1973) 99–144.
[21] D.H. Harris, M.F. Lappert, J. Chem. Soc., Chem. Commun. (1974) 895–896.
[22] M. Veith, Angew. Chem. 87 (1975) 278–288.
[23] M. Veith, F. Goffing, V. Huch, Z. Naturforsch. 43b (1988) 846–856.
[24] (a) W.A. Herrmann, M. Denk, J. Behm, W. Scherer, F.-R. Klingan, H. Bock, B. Solouki, M. Wagner, Angew. Chem., Int. Ed. Engl. 31 (1992) 1485–1488;
(b) M. Denk, R. Lennon, R. Hayashi, R. West, A. Belyakov, H.P. Verne, A. Haaland, M. Wagner, N. Metzler, J. Am. Chem. Soc. 116 (1994) 2691–2692;
(c) A. Dhiman, T. Müller, R. West, J.Y. Becker, Organometallics 23 (2004) 5689–5693.
[25] M.F. Lappert, S.J. Miles, P.P. Power, A.J. Carty, N.J. Taylor, J. Chem. Soc., Chem. Commun. (1977) 458–459.
[26] M.F. Lappert, R.S. Rowe, Coord. Chem. Rev. 100 (1990) 267–292.
[27] T.A.K. Al-Allaf, C. Eaborn, P.B. Hitchcock, M.F. Lappert, Chem. Commun. (1985) 548–549.
[28] S.L. Ellis, P.B. Hitchcock, S.A. Holmes, M.F. Lappert, M.J. Slade, J. Organomet. Chem. 444 (1993) 95–99.
[29] M. Veith, L. Stahl, V. Huch, Inorg. Chem. 28 (1989) 3278–3279.
[30] M. Veith, S. Becker, V. Huch, Angew. Chem., Int. Ed. Engl. 28 (1989) 1237–1238.
[31] M. Veith, S. Becker, V. Huch, Angew. Chem., Int. Ed. Engl. 29 (1990) 216–218.
[32] M.C. Kuchta, G. Parkin, J. Chem. Soc., Chem. Commun. (1994) 1351–1352.
[33] M.C. Kuchta, G. Parkin, J. Am. Chem. Soc. 116 (1994) 8372–8373.
[34] M.C. Kuchta, T. Hascall, G. Parkin, J. Chem. Soc., Chem. Commun. (1998) 751–752.
[35] Y. Zhou, D.S. Richeson, J. Am. Chem. Soc. 118 (1996) 10850–10852.
[36] S.R. Foley, C. Bensimon, D.S. Richeson, J. Am. Chem. Soc. 119 (1997) 10359–10363.
[37] S.R. Foley, G.P.A. Yap, D.S. Richeson, Organometallics 18 (1999) 4700–4705.
[38] S.R. Foley, G.P.A. Yap, D.S. Richeson, J. Chem. Soc., Dalton Trans. (2000) 1663–1668.
[39] W.-P. Leung, W.-H. Kwok, L.T.C. Law, Z.-Y. Zhou, T.C.W. Mak, Chem. Commun. (1996) 505–506.
[40] W.-P. Leung, W.-H. Kwok, Z.-Y. Zhou, T.C.W. Mak, Organometallics 19 (2000) 296–303.
[41] G. Ossig, A. Meller, C. Brönneke, O. Müller, M. Schäfer, R. Herbst-Irmer, Organometallics 16 (1997) 2116–2120.
[42] N. Tokitoh, M. Saito, R. Okazaki, J. Am. Chem. Soc. 115 (1993) 2065–2066.
[43] Y. Matsuhashi, N. Tokitoh, R. Okazaki, Organometallics 12 (1993) 2573–2583.
[44] N. Tokitoh, T. Matsumoto, K. Manmaru, R. Okazaki, J. Am. Chem. Soc. 115 (1993) 8855–8856.
[45] T. Matsumoto, N. Tokitoh, R. Okazaki, Angew. Chem., Int. Ed. Engl. 33 (1994) 2316–2317.
[46] H. Suzuki, N. Tokitoh, T. Matsumoto, S. Nagase, R. Okazaki, J. Am. Chem. Soc. 116 (1994) 11578–11579.
[47] N. Tokitoh, T. Matsumoto, R. Okazaki, J. Am. Chem. Soc. 119 (1997) 2337–2338.
[48] M. Saito, N. Tokitoh, R. Okazaki, J. Am. Chem. Soc. 119 (1997) 11124–11125.
[49] H. Suzuki, N. Tokitoh, R. Okazaki, S. Nagase, M. Goto, J. Am. Chem. Soc. 120 (1998) 11096–11105.
[50] N. Tokitoh, T. Matsumoto, R. Okazaki, Bull. Chem. Soc. Jpn. 72 (1999) 1665–1684.
[51] T. Matsumoto, N. Tokitoh, R. Okazaki, J. Am. Chem. Soc. 121 (1999) 8811–8824.
[52] R. Okazaki, N. Tokitoh, Acc. Chem. Res. 33 (2000) 625–630.
[53] T. Tajima, N. Takeda, T. Sasamori, N. Tokitoh, Organometallics 25 (2006) 3552–3553.
[54] T. Chivers, T.J. Clark, M. Krahn, M. Parvez, G. Schatte, Eur. J. Inorg. Chem. (2003) 1857–1860.
[55] T. Chivers, D.J. Eisler, J.S. Ritch, Z. Anorg. Allg. Chem. 630 (2004) 1941–1946.
[56] D.J. Eisler, T. Chivers, Chem. Eur. J. 12 (2006) 233–243.
[57] Although the "double-bond rule" is often cited in this context, it has never been stated explicitly as a rule in printed form. For a more detailed discussion, see Ref. [64].
[58] L. Pauling, The Nature of the Chemical Bond, third ed., Cornell University Press, Ithaca, 1960.
[59] I. Schranz, L. Stahl, R.J. Staples, Inorg. Chem. 37 (1998) 1493–1498.
[60] Attempts to refine the structure as a pseudo-merohedrally, cubically twinned, orthorhombic crystal of space group *Pbca* failed. The refinement was not stable.
[61] For a discussion of this phenomenon, see also: M. Chakravarty, P. Kommana, K.C. Kumara Swamy, Chem. Commun. (2005) 5396–5398.
[62] Manuscript in preparation.
[63] P.B. Hitchcock, E. Jang, M.F. Lappert, J. Chem. Soc., Dalton Trans. (1995) 3179–3187.
[64] M.C. Kuchta, G. Parkin, Coord. Chem. Rev. 176 (1998) 323–372.
[65] J. Kapp, M. Remko, P.v. Ragué Schleyer, J. Am. Chem. Soc. 118 (1996) 5745–5771.
[66] Parkin has noted that for transition metal chalcogenides the tendency to dimerize is exactly reversed, and that this is likely due to the greater polarity of the Group 14 element-to-chalcogen bond. See Ref. [34].
[67] The Ge=E moities shown were obtained from compounds Ge–O (**2**), Ge=S (**3**), Ge=Se (**F**), and Ge=Te (**F**). The germanium–oxide bond is a bridging bond, and the van der Waals radius may therefore be somewhat smaller than if it had been a terminal Ge=O bond.
[68] H. Stephen, J. Chem. Soc. (1930) 2786–2787.
[69] SMART V 4.043 Software for the CCD Detector System, Bruker Analytical X-ray Systems, Madison, WI, 1995.
[70] SAINT V 4.035 Software for the CCD Detector System, Bruker Analytical X-ray Systems, Madison, WI, 1995.
[71] SADABS program for absorption corrections using the Bruker CCD Detector System. Based on: R. Blessing, Acta Crystallogr. Sect. A: Found. Crystallogr. A 51 (1995) 33–38.
[72] G.M. Sheldrick, SHELXS-90Program for the Solution of Crystal Structures, University of Göttingen, Germany, 1990.
[73] G.M. Sheldrick, SHELXL-97Program for the Solution of Crystal Structures, University of Göttingen, Germany, 1997.
[74] SHELXTL 5.10 (PC-Version), Siemens Analytical X-Ray Instruments, Inc. Madison, WI, 1998.
[75] E.J. Gabe, Y. Le Page, J.-P. Charland, F.L. Lee, P.S. White, J. Appl. Crystallogr. 22 (1989) 384.